Statistical and hydrodynamic numerical modeling to quantify storm surge hazard: Comparison of approaches applied to U.S. North Atlantic coast

Yasser Hamdi, Norberto C. Nadal-Caraballo, Joseph Kanney, Meredith L. Carr, Vincent Rebour

Weather and Climate Extremes 42 (2023) 100628

Contents lists available at ScienceDirect

Weather and Climate Extremes

journal homepage: www.elsevier.com/locate/wace

Statistical and hydrodynamic numerical modeling to quantify storm surge hazard: Comparison of approaches applied to U.S. North Atlantic coast

Yasser Hamdi [a,*], Norberto C. Nadal-Caraballo [b], Joseph Kanney [c], Meredith L. Carr [b], Vincent Rebour [a]

[a] Institute for Radiological Protection and Nuclear Safety, 31 Av. De La Division Leclerc, 92262, Fontenay-Aux-Roses, France
[b] U.S. Army Coastal and Hydraulics Laboratory, 3909 Halls Ferry Road, Vicksburg, MS, 39180, USA
[c] U.S. Nuclear Regulatory Commission, Washington, DC, 20555-0001, USA

ARTICLE INFO

Keywords:
Tropical cyclones
Extratropical storms
Storm surge
Frequency analysis
Probabilistic coastal hazards analysis
Multivariate flood hazard analysis

ABSTRACT

Estimating the storm surge magnitude and annual exceedance probability is a key element in the siting and design of coastal nuclear power plants in both the U.S. and France. However, differences in storm climatology, specifically the relative importance of tropical cyclones (TCs) versus extratropical storms (XTCs), have driven differences in estimation method development. This work compares purely statistical modeling with combined statistical and numerical simulation modeling approaches for extreme storm surge applied to the U.S. North Atlantic coast which is subject to both tropical and extratropical storms. Two frequency analysis methods are applied to observed water levels and compared to a copula-based joint probability analysis of TCs and automated frequency analysis of XTCs that is enriched with numerically simulated storms. One frequency analysis method is applied using (1) hourly at-site data and (2) hourly at-site data enriched with additional data from a homogeneous region. The other frequency analysis method is applied using (1) hourly at-site data and (2) hourly at-site data enriched with monthly water level maxima. Variables of interest used in the comparison are skew storm surge, maximum instantaneous storm surge, non-tidal residual and maximum seal level. The performance of the methods (mean surge and water level estimates and confidence intervals) depend on the variable of interest and, to some extent, on return period. Inclusion of additional information (e.g., regional water levels, and monthly maxima) in the frequency analysis methods does not have a large impact on estimated mean surge and water levels, but significantly reduces resulting confidence intervals (over 40% reduction in some cases). However, the confidence intervals still grow with increasing return period. Inclusion of simulated storms in the joint probability analysis results in significantly different mean surge and water level estimates (up to 25% higher than the frequency analysis in some cases). The joint probability analysis confidence intervals are wider than those for the frequency analysis methods lower return periods (e.g., 60%–80% wider at 100 years), but they grow much more slowly and are significantly narrower for higher return periods (e.g., 40%–60% narrower at 1 000 years). Although there are appreciable differences between the results documented in this paper, these are reasonable due to differences in the data and methods used in this comparison.

1. Introduction

Storm surge due to tropical cyclones (TCs) and extratropical storms (XTCs) have serious environmental, economic, and social consequences (Lin et al., 2010; Orton et al., 2019; Yin et al., 2017). During the last three decades, the United States of America (U.S.) and France have experienced violent storms. Notable landfalling TCs on the U.S. Atlantic and Gulf coasts include Katrina (2005), Sandy (2012), Harvey (2017), Maria (2017), Laura (2020), and Ian (2022) (Knobby et al., 2023; Blake et al., 2013; Blake and Zelinksy, 2018; Pasch et al., 2021, 2023; Bucci et al., 2023). Significant extratropical storms impacting the French Atlantic coast include Martin (1999), Klaus (2009) and Xynthia (2010) (Ulbrich et al., 2001; Liberato et al., 2011, 2013). Mixed storms such as TCs that transition to XTCs can also produce large surge and flooding (Orton et al., 2015). The impact of TCs, XTC and mixed storms is expected to increase with rising sea levels (Lin et al., 2016; Yin et al.,

* Corresponding author.
E-mail address: Yasser.Hamdi@ised-isde.gc.ca (Y. Hamdi).

https://doi.org/10.1016/j.wace.2023.100628
Received 27 March 2023; Received in revised form 8 November 2023; Accepted 14 November 2023
Available online 18 November 2023

2017). With this in mind, staff of the U.S. Nuclear Regulatory Commission (NRC) has collaborated with staff of the U.S. Army Corps of Engineers, Engineer Research and Development Center, Coastal and Hydraulics Laboratory (USACE), and the French Institute for Radiological Protection and Nuclear Safety (IRSN) to investigate probabilistic approaches and methods that can more comprehensively and consistently capture the effects of low probability events given the existing observational data.

Critical infrastructure in coastal areas, such as nuclear power plants, should be designed and operated withstand flooding hazards from extreme storms. However, systematic storm observations are often limited due to relatively short record lengths, gaps during extreme events caused by instrumentation failure, and low spatial resolution (e.g., sparse gauging stations) and temporal resolution (e.g., low TC occurrence frequency). Subsequently, commonly used deterministic and statistical estimation methods may have large uncertainties and not properly capture some exceptional events (Aerts et al., 2013; Lin et al., 2010; Orton et al., 2015, 2016). Some local surges induced by exceptional storms appear as outliers, especially if concurrent with another phenomenon such as high tides and waves.

Probabilistic storm surge models coupling statistical methods with accurate, high-resolution hydrodynamic numerical models for TC and XTC storm surge, such as joint probability analysis integrated with coupled wind-wave-surge models, have provided a more comprehensive theoretical approach to extreme surge estimation. This approach requires the development of a joint probability model linking storm or atmospheric forcing (e.g., storm size, intensity, forward translation speed, landfall location for TCs) and storm responses such as storm surge, total water level, waves (Vickery et al., 2000; Powell et al., 2005; Emanuel et al., 2006; Rumpf et al., 2007; Hall and Jewson, 2007; Lin et al., 2010; Nadal-Caraballo et al., 2015a, 2022; Lopeman et al., 2015; Gonzalez et al., 2019; Orton et al., 2019).

The USACE has conducted several regional studies on the U.S. coastline which have evolved methods for TCs and XTCs (USACE, 2009, 2011; Melby et al., 2012; Nadal-Caraballo et al., 2012). Statistical analysis of water levels to obtain first order estimates of return periods and magnitudes of water levels recorded at locations from Virginia to Maine were included in Phase I of the North Atlantic Coastal Comprehensive Study (NACCS, Nadal-Caraballo and Melby, 2014; Nadal-Caraballo et al., 2015b). The results from this analysis exhibited limitations primarily arising from mixed storm populations and underrepresentation of TCs. NACCS Phase II comprised joint probability method (JPM) regional statistical analysis, high-fidelity numerical hydrodynamic modeling performed for TCs and an improved frequency analysis for XTCs (Nadal-Caraballo et al., 2015a). USACE subsequently developed the Coastal Hazards System (CHS) probabilistic framework in collaboration with the University of Notre Dame (Nadal-Caraballo et al., 2022), which incorporates a detailed dependence structure correlating the TC atmospheric-forcing parameters, an optimal sampling process, the bias correction, and uncertainty estimation (Nadal-Caraballo et al., 2022). The CHS framework addresses XTCs through the Stochastic Simulation Technique (SST), an improved peaks over threshold (POT)-based frequency analysis method with automated threshold selection (Yawn et al., 2023). It addresses TCs using Joint Probability Method Aided by Metamodel Prediction (JPM-AMP), an improved joint probability method incorporating multivariate copulas to develop joint distributions for atmospheric forcing parameters and machine learning to emulate hydrodynamic TC responses. These methods have been applied to the U.S. North Atlantic region in the 2023 update of the NACCS study (CHS-NA-2023) and the results for the New York region are used in this paper.

IRSN has conducted studies focused on the French Atlantic coast, which is subject to extratropical and post-tropical storms, and developed statistical models for storm surge that include: (1) local frequency analysis (FA); (2) regional FA inspired by the theory of Hosking and Wallis (Hosking and Wallis, 1997; Bardet et al., 2011); and (3) target-site-based regional frequency modeling (TS-RFM). TS-RFM weights both local and regional effects, using an empirical spatial extremogram (ESE) to define a homogenous region of interest centered on the target-site (Hamdi et al., 2019). TS-RFM transfers data from the homogeneous region to enrich the target-site record. The storm surges at the target-site are reconstituted from those of homogeneous region sites using multiple linear regression (MLR), providing an optimized local set of events representative for the target-site (not the region, as in the Hosking and Wallis approach). A further noteworthy feature of the TS-RFM is that it can easily incorporate the historical information, which herein refers to information derived from observations occurring outside the period of systematic measurements. Use of historical information in the TS-RFM model significantly improves estimations when dataset contain statistical outliers (Hamdi et al., 2015; Saint-Criq et al., 2022). However, since the use of historical information is not the focus of this study, this feature of the model was not applied.

As previously noted, the study region is subject to mixed storm populations including XCs, TCs, and hybrid storms such as TCs that transition to XTCs. However, the TS-RFM and SST statistical approaches used in this paper operate on water levels, and thus do not directly account for storm type. The JPM-AMP approach assesses XC and TC populations separately, and indirectly accounts for hybrid storms by generating synthetic TCs with atmospheric parameters (e.g., storm size and translation speed) in ranges characteristic of the hybrid population.

The objective of this work is to compare the approaches discussed above in coastal settings that are subject to both tropical and extratropical surges. Specifically, the TS-RFM method (with and without regional information) are compared to the SST and JPM-AMP methods. The results are expressed in terms of annual exceedance frequency (AEF) and return level. The paper is structured as follows: In section 2, the data used and variables of interest are presented and then estimation methods are described. Section 3 describes application of the methods for a location on the U.S. North Atlantic coast and presents the resulting inferences. The results are compared and discussed in section 4. Conclusions and perspectives are provided in section 5.

2. Data and methods

2.1. Supporting data and variables of interest

The coastal region considered experiences both XTCs and TCs. TCs are localized rotating intense low-pressure systems and TC-generated surge can generally be modeled using a small set of meteorological parameters (see section 3.1.2). XTCs are very rarely well defined in space (e.g., uniform, symmetrical) and cannot be efficiently characterized by a small meteorological parameter set. Water level measurements form the basis for most statistical XTC surge models.

Multiple data sources were used in this study. The U.S. National Oceanic and Atmospheric Administration (NOAA) maintains a network of tide gage stations and provides water level records and tide predictions for the U.S. coastal regions (https://tidesandcurrents.noaa.gov). The NOAA National Hurricane Center (NHC) maintains the HURDAT2 (HURricane DATa 2nd generation) database, comprising reanalysis data for North Atlantic basin TCs (i.e., North Atlantic Ocean, Gulf of Mexico, and the Caribbean Sea) from 1851 to the present,

Table 1
Data and periods of records used in this study.

Organization	Analysis Method	Data Type	Period of Record
IRSN	TS-RFM	observed hourly water levels	1902–2013
USACE	SST	observed hourly and monthly water levels	1902–2013
	JPM-AMP	TC observations (HURDAT2)	1938–2021
		XTC water level records	1938–2013

(Langousis et al., 2016; https://www.nhc.noaa.gov/data/). The data used, spanning the years 1902–2021, are summarized in Table 1 and Fig. 1.

Storm surge, a rise in sea level due to low atmospheric pressure and strong winds, is the main driver of coastal flooding hazards and the focus of this paper. Wind wave effects are not analyzed here, so hourly observed still water level time series data are the basic input to each method discussed. In this paper the terms water level and sea level are used interchangeably. The mean linear trend in the time series is subtracted from the hourly water levels to produce a detrended time series prior to computation of any variable of interest. This removes effects such as long-term sea level change due to climate change, tectonic movement, and other influences. The variables of interests in this study are defined as follows.

- Nontidal residual (NTR): the difference between the observed water level and the corresponding predicted peak at the same timestamp.
- Maximum instantaneous storm surge (MISS): the largest NTR between successive high tides.
- Skew storm surge (SSS): the difference between the maximum observed sea level and the maximum predicted peak water level inside a time window and regardless of their timing during the tidal cycle.
- Maximum observed sea level (MaxSL): the maximum observed water level in each tidal cycle.
- Combined MaxSL: combined series comprising POT observed hourly water levels and maximum monthly water levels with duplicates removed.

2.2. SST and JPM-AMP methods

USACE employed three methods in this study to assess the water level hazard at The Battery, New York, U.S.: (1) SST using hourly observations from mixed storm populations; (2) SST using hourly observations enriched with monthly data to expand the data set; and (3) CHS framework using the NACCS Phase II atmospheric and hydrodynamic modeling results but combining JPM-AMP for TCs and improved SST for XTCs (results will be referred to as JPM-AMP).

2.2.1. SST method for mixed TC/XTCs

The SST replaces the Empirical Simulation Technique (EST) developed by USACE in the 1990s for conducting storm surge frequency analysis (Borgman et al., 1992; Scheffner et al., 1999). SST fits a Generalized Pareto Distribution (GPD) to improve estimation of the low-frequency tail using a novel automated threshold selection approach inspired by Langousis et al. (2016). Similar to EST, the SST uses an empirical distribution to fit the high-frequency observations below the GPD threshold. When conducting a peaks-over-threshold (POT) analysis of observations, it has been shown that, for a high enough threshold and a large enough average number of threshold exceedances (λ_{POT}), the distribution for the excess converges to a GPD (Pickands, 1975). There is no general equation for selecting the GPD threshold, so graphic methods (i.e., parameter stability plots) have been used, with differing degrees of success. In the mean residual life (MRL) graphical approach (Coles, 2001), the mean of the excesses is plotted against possible GPD thresholds, and the optimal threshold corresponds to the lowest threshold on the linear section of the plot. However, identification of a unique optimal threshold can be difficult and led to the development of the SST automated threshold detection method based in that described by Langousis et al. (2016) and enhanced by local climatology information on extreme events.

In this approach, multiple viable thresholds are identified along with their corresponding thresholds storm sample rates (λ_{th}). A climatological target storm sample rate (λ_c), defined as the expected number of storm events sampled per year based on regional climatology, is an additional criterion when selecting the GPD threshold (e.g., threshold closest to $\lambda_c = 2$ events per year). SST confidence intervals (CIs) are estimated by repeated (e.g., 100 times) non-parametric bootstrapping with replacement.

SST is also used in the CHS framework, as discussed next, for assessing the hazard due to numerically modeled XTCs.

2.2.2. Coastal Hazards System (CHS) framework with JPM-AMP

The CHS framework with JPM-AMP (Nadal-Caraballo et al., 2022; 2022) was developed to overcome limitations of previous JPM studies, which typically relied on coarse storm sampling and lacked joint probability models that incorporated storm parameter correlations, geospatial quantification of bias and uncertainty, and bias correction. JPM-based frameworks comprise several key steps to quantify storm surge and other coastal hazards. The main components of the CHS framework and their interconnection are illustrated in Fig. 2.

For TCs, tasks include statistical quantification of regional storm climatology, constructing one or more regional joint distribution models for storm characteristics, efficiently sampling from them to generate synthetic TCs spanning the parameter and probability space, and then modeling the synthetic storms from basin scale down to local scale using high-fidelity hydrodynamic ocean process models. Recent JPM-AMP advancements for the assessment of TC-driven hazards are outlined in red in Fig. 2, and briefly described below.

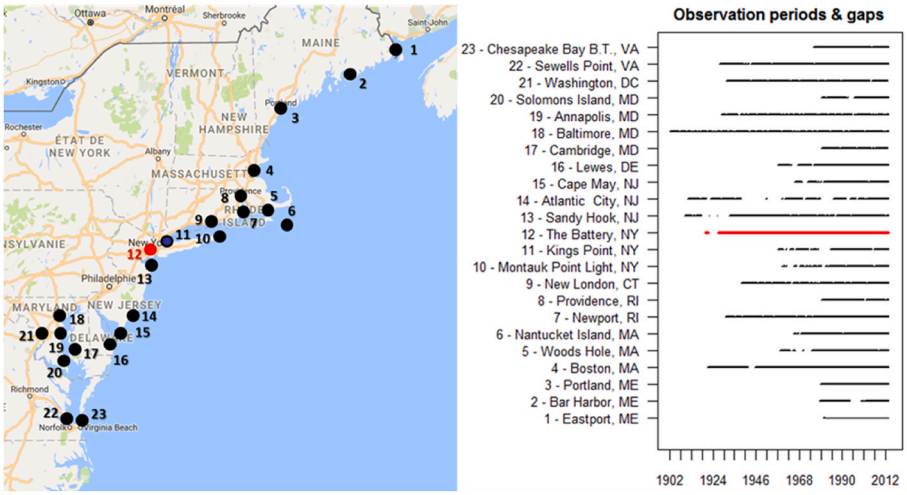

Fig. 1. NOAA tide gage locations (left); data record at each gage (right).

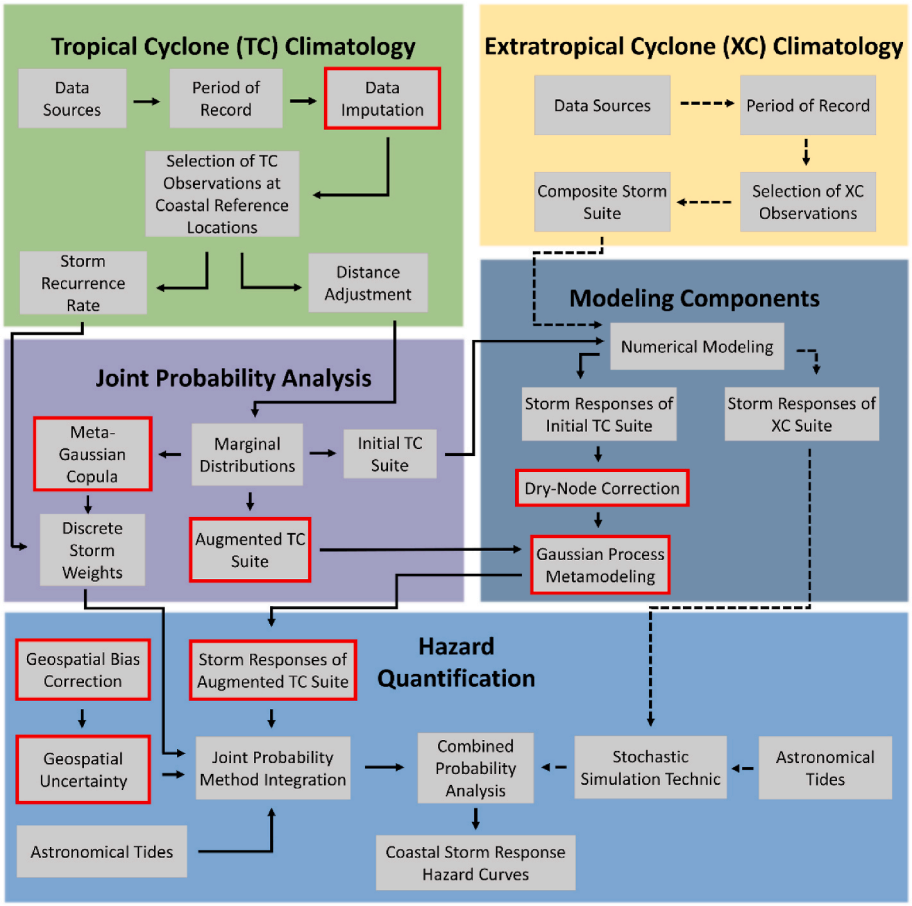

Fig. 2. Main components of the USACE CHS framework. JPM-AMP enhancements outlined in red.

1) Fill gaps in the HURDAT2 Δp data and incorporate $R_{\max}$ estimates using Gaussian process metamodeling in a data imputation process to expand the historical record of these parameters.
2) Develop a meta-Gaussian copula joint probability model, explicitly accounting for the correlation between TC atmospheric parameters.
3) Refine the initial TC suite, informed by the meta-Gaussian copula model, to develop an augmented TC suite for improved definition of the atmospheric-forcing parameter space.
4) Perform dry node correction to fill missing storm surge values and complete the surge surface over the required domain.
5) Train and apply Gaussian process metamodeling to generate storm surge responses for the augmented TC suite while retaining the high-fidelity nature of the initial TC suite hydrodynamic simulations.
6) Quantify geospatial bias and uncertainty and perform bias correction.

2.2.2.1. JPM-AMP for TCs. As used in the CHS framework, the JPM integral (without the error term) used to develop TC response hazard curves, which is presented in Nadal-Caraballo et al. (2015b), takes the following form:

$$\lambda_{\tau_{max}>\tau} = \lambda \int P[\tau_{max}(\widehat{x}) > \tau|\widehat{x}] f_{\widehat{x}}(\widehat{x}) d\widehat{x}$$

$$\approx \sum_{i}^{n} \widehat{\lambda}_i P[\tau_{max}(\widehat{x}_i) > \tau|\widehat{x}_i] \quad (1)$$

where $P[\tau_{max}(\widehat{x}) > \tau|\widehat{x}]$ represents the conditional probability that a storm response $\tau_{max}(\widehat{x})$ produces a response greater than τ given the atmospheric-forcing vector $\widehat{x}$ and $\lambda_{\tau_{max}>\tau}$ = annual exceedance frequency (AEF) of TC response $\boldsymbol{\tau}$ due to $\widehat{x}$; λ = storm recurrence rate (storms/year/km); and n = number of TCs. In the discrete JPM integral, $\widehat{\lambda}_i$ is defined as the discrete storm weight of the i-th synthetic TC, where $\widehat{\lambda}_i = \lambda p_i$, and p_i is the product of its discrete joint probability (i.e., normalized probability densities) and the spacing between synthetic TC tracks defined in the JPM. This form of the JPM integral does not include the error term, as uncertainty is conveyed through non-exceedance confidence limits (CLs) which capture the total uncertainty associated with atmospheric and hydrodynamic modeling errors.

In the CHS framework, multivariate copulas are applied to establish relationships between TC parameters. Copulas are dependence functions that link marginal distributions to form a unique joint probability distribution (Sklar, 1959). Specifically, meta-Gaussian copulas (Zhang and Singh 2019) are used to further discretize the initial TC suite parameter and probability spaces in order to develop an augmented TC suite with a significantly higher density of synthetic storms. Relationships between the atmospheric forcing vector in the JPM equation and TC responses (e.g., storm surge, SWL, wave climate) were established using a machine learning technology called Gaussian process metamodeling (Jia et al., 2016; Zhang et al., 2018). The application of metamodeling in the context of a JPM-based study facilitated development of an augmented TC suite of more than 1 million storms, along with the prediction of corresponding hydrodynamic responses. All augmented TC suite responses along with their discrete storm weights are aggregated to compute the AEF of each storm response. The reader is referred to Nadal-Caraballo et al. (2015b, 2022) for more details on the JPM integral and TC-response hazard curve development process.

2.2.2.2. SST method for XTCs. The CHS frameworks applied the SST

method to conduct FA of XTC hazards for the CHS-NA update. Instead of relying on XTC observations, the CHS framework relied on the high-fidelity numerical model results corresponding to the XTCs, as simulated during NACCS Phase II. In that study, extreme XTCs were sampled from water level observations prior to conducting simulations using high-fidelity models. To select the XTCs to be modeled and subsequently assessed using the SST method, an optimized regional set of events was constructed to be representative of the entire NACCS area, using the composite storm set method (Nadal-Caraballo et al., 2012). General steps in this method are.

1) Evaluate POTs for selected tide gage records to identify local peaks (select representative gages to uniformly cover the region).
2) At each gage, isolate the XTC population, called the full storm set, by eliminating TCs, convective storms, and other non-wind driven events using meteorological information.
3) Fit a GPD to the full storm set at each gage.
4) Testing different numbers of storms, iteratively develop the composite storm set, a minimal set of the highest values from each gage which best matches the full storm set GPDs.
5) Validate the composite set by comparing to the full storm set water levels over a range of high to low AEFs (e.g., by comparing the root mean square deviation error between composite and full storm distributions)

The storms that constitute the composite set were then simulated using atmospherically and hydrodynamic numerical modeling (i.e., hindcast wind and pressure fields used to reconstitute storm surges and wave characteristics), to estimate XTC responses over the entire CHS-NA region. The XTC FA was conducted using the numerical simulation results of the composite storm set as input to SST, which was previously discussed in Section 2.2.1.

The final water level hazard curves JPM-AMP hazard curves developed part of the CHS-NA update integrate the results from the application of both JPM-AMP for TCs and SST for XTCs. The recent advancements of the CHS framework with JPM-AMP resulted in more robust hazard curves that better represent the local storm climatology and resulting hydrodynamic responses.

2.3. IRSN TS-RFM method

The main objective of the IRSN in this work was to estimate the extreme sea levels and associated uncertainties at U.S. North Atlantic coast target-sites using the IRSN-developed TS-RFM.

The open-source R software environment for statistical computing (available at www.r-project.org) was used to conduct the calculations detailed in this report. Frequency estimations were performed with the IRSN-developed Renext library, an extremal FA package specifically developed for flood frequency analyses using the POT method. Details on features of the Renext library are provided in Hamdi et al. (2014, 2015).

TS-RFM was applied to same U.S. North Atlantic coast region and 23 gages used in the USACE NACCS with the Battery (NY) and Kings-Point (NY) as a target-sites, although only results for the Battery will be discussed herein. The peaks-over-threshold using historical information (POTH) as described in Hamdi et al. (2015) can use regional as well as historical information, although only regional information is used in this study.

The general steps TS-RFM include.

- Identify the region, sites (gages) within the region, and the site of interest (target site);
- Define the variable of interest (IRSN typically uses skew storm surge);
- Collect historical information (e.g., literature, archives, etc.);
- Collect and analyze systematic data (observations);
- Extract independent and identically distributed extremes at all the sites in the region;
- Define model settings (e.g., extreme quantiles, the neighborhood threshold, effective duration);
- Compute the Empirical Spatial Extremogram (ESE) with the pairwise extremal dependence between target-site and all the sites in the region to form the homogenous region;
- Transfer regional information to the target-site using the MLR approach;
- Decluster observations and find optimal POTH threshold;
- Perform the local FA using regional (and historical information if available) with the POTH to estimate quantiles and CIs.

The TS-RFM transfers regional information from neighboring sites located in a homogeneous region to the site of interest (target site). The ESE is used to form a homogenous region of interest centered on this target-site. The pairwise extreme surges or sea levels used to compute the ESE are often induced simultaneously by the same storms, so declustering is required to maintain spatial independence of events. Regarding the extreme surge definition and extraction, the 99% quantile is selected as a sufficiently high threshold above which a surge is considered extreme. Additional details on threshold selection are discussed in Hamdi et al. (2018) and an additional example of ESE application is provided in Andreevsky et al. (2020). It is interesting to note that the TS-RFM approach provides an optimized local-regional set of events that is representative of the target-site, not the region and it can easily incorporate historical information (i.e., observations other than systematic gage records).

Once regional information is transferred to the target-site, a long and much more complete local dataset is obtained, and a local FA can be conducted. The regional extreme surges, which have joined the target-site series, can potentially play a useful and major role in the construction of the body of the sample of extreme surges, and then reinforce the statistical fitting at the bulk of the distribution and at the upper tail as well. Of the many statistical distributions commonly used for extremes, the GPD is the most suitable theoretical distribution to fit observations. It calculates probabilities of observing extreme events which are above a sufficiently high threshold. The use of a high threshold (provided that the sample size remains reasonable) provides a sample that is more representative of extreme events. Several studies show that, when the selected threshold u is sufficiently high, the asymptotic form of the distribution function for the excess converges to a GPD (Pickands, 1975).

Confidence intervals are calculated use the delta method, which assumes an asymptotic approximation to a gaussian distribution (Hamdi et al., 2014).

3. Application of methods to U.S. North Atlantic coast location

This section summarizes and compares results obtained when applying the SST, JPM-AMP and TS-RFM methods to The Battery, NY.

3.1. Application of SST

For this study, hourly observations at The Battery, New York were used to produce a POT dataset inclusive of TCs and XTCs. SST was used to provide a baseline FA-type assessment of the water level hazard. To demonstrate the use of additional information to assess the water level hazard, water level POT series from both hourly and monthly maxima data sets were merged and duplicate events eliminated, prior to conducting the SST FA.

The SST method with automated threshold selection was used to perform a frequency analysis considering the mixed-population (i.e., TCs and XTCs) storm surge and water levels (SSS, NTR, MaxSL, and combined MaxSL) observed at The Battery, NY. The default SST POT rate (λ_{POT}) was set at 12 events/year to include events covering a wide range

of probabilities, including high-frequency events that are used in beach morphology analyses. Empirical estimates as low as 2 events/year were considered and tested for sensitivity. Results for The Battery, NY (mean hazard curve with the 70% and 90% CIs) are shown in Fig. 3. As previously discussed, the SSS and NTR variables constitute two different approaches to represent storm surge. Fig. 3 shows that NTR yields larger estimates of storm surge relative to SSS. Fig. 3 also shows that combining hourly observations and monthly maxima data (Comb MaxSL) significantly reduced the CI widths and the mean hazard curve is shifted to the right with reduced slope.

3.2. Application of JPM-AMP

The JPM with optimal sampling approach used in NACCS Phase II evolved into the CHS framework with JPM-AMP via advancements such as copula-based probabilistic analysis and machine learning techniques. To quantify water level hazards in due to TCs in the U.S. North Atlantic region, the CHS-NA update employed JPM-AMP and leveraged the initial TC suite of 1 050 synthetic storms developed for NACCS Phase II, as well as the original high-fidelity numerical simulations carried out for that study.

The CHS results presented herein were developed as part of the North Atlantic update (CHS-NA-2023) of the NACCS effort previously discussed. Results were developed using the CHS framework with JPM-AMP for the joint probability analysis of synthetic TCs and SST method for the frequency analysis of XTC simulation results. The JPM-AMP results from virtual gage 230,889 of CHS-NA-2023 (near The Battery, NY) plotted in Fig. 4 show hazard curves that perform better than the standalone-SST frequency analysis results at low frequencies, with a more realistic shape that is not so concave up. Note that the JPM-AMP hazard curve confidence limits account for the epistemic uncertainty associated with numerical model errors of the JPM approach and are not estimated from bootstrapping or stochastic uncertainty of the parameters used in distribution fitting.

3.3. Application of TS-RFM

The TS-RFM approach was applied at the Battery for three variables of interest: SSS, MISS and MaxSL. Results of the homogenous region delineation and the transfer of regional information to the target-site are discussed first. Then the frequency estimates and diagnostics are presented in probability plots and tables.

3.3.1. Homogeneous regions delineation

Fig. 5 shows the pairwise extremal dependence coefficient between the target and regional sites, along with the resulting homogeneous regions for the Battery, NY. Coherent regions of interest (corresponding to a neighborhood threshold of 0.4 for all the variables of interest) are obtained from the ESE based on the pairwise extremal dependence coefficient χ between the Battery and all the sites in the region. One obtains almost the same homogenous regions for SSS, MISS and MaxSL variables.

3.3.2. Transfer of regional information to the target-site

Regional information was transferred from the homogenous region to the target-site using a MLR model. A regression matrix merging all the data tables at neighboring sites was constructed. The set of effective sites (sites for which the merged record has no gaps) which varied with time was used to compute correlation coefficients between the target-site and its neighbors (see Fig. 6). These correlations were analyzed to identify the most influential sites in the homogeneous region and to identify the sites with very low correlations (<0.3) with target-site. Correlation coefficients give a preliminary idea about which sites are consistent and provide a measure of the pairwise linear relation between target and neighboring sites' explanatory variables. This step also indicates the existence of collinearities between them. Sites with relatively low correlations are not automatically eliminated from the inference. An analysis of variance (ANOVA) technique was subsequently performed to keep or remove them from the transfer procedure.

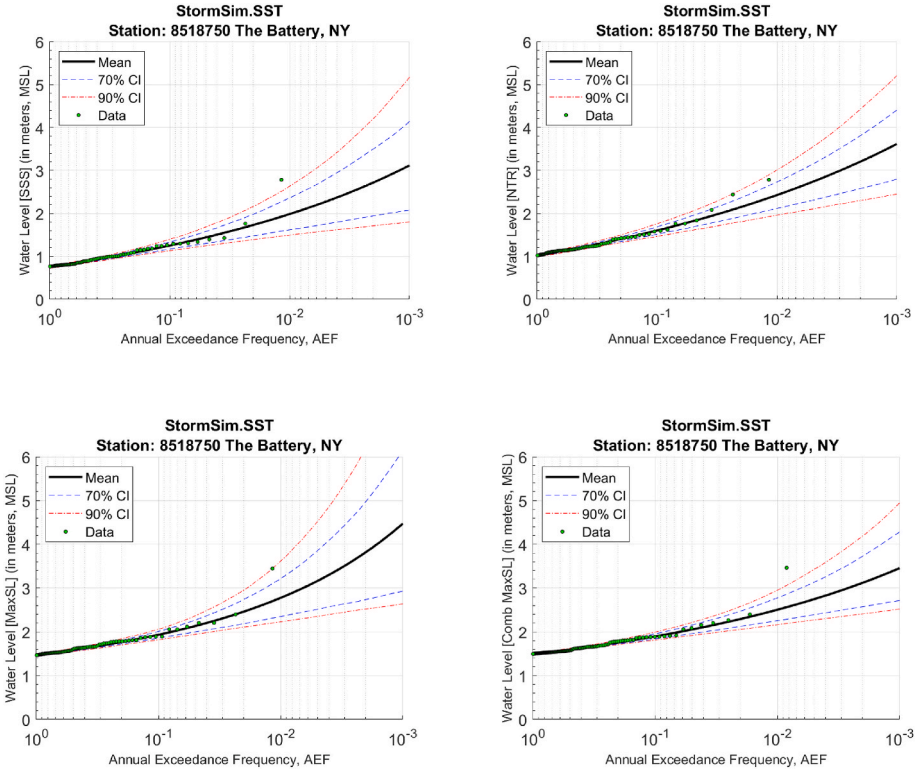

Fig. 3. SST results for The Battery, NY: SSS (top left), NTR (top right), maximum sea level from hourly observations (bottom left), and maximum sea level combining hourly observations and monthly maxima data (bottom right).

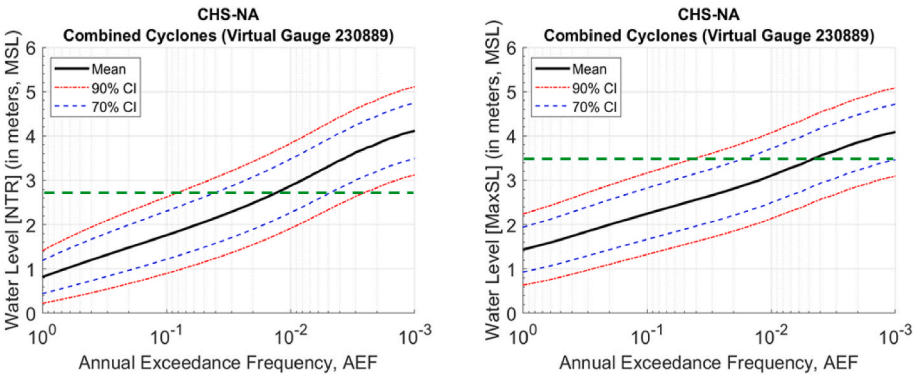

Fig. 4. JPM-AMP results for virtual gage 230,889 (The Battery, NY) for NTR (left) and MaxSL (right). For comparison, empirical estimate for hurricane Sandy water levels as green dashed line.

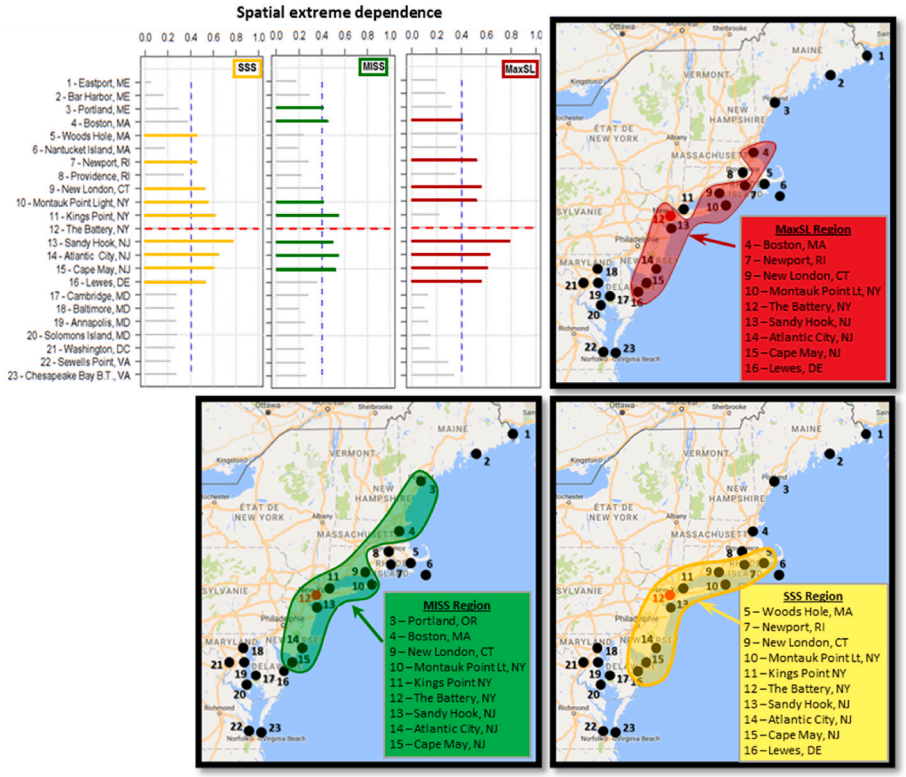

Fig. 5. Pairwise extremal dependence coefficients and resulting homogeneous regions for the Battery, NY target site.

Regional regressions were also examined. The statistical significance of each regression model was analyzed using root-mean-square error (RMSE) and the Nash–Sutcliffe (NS) coefficient for each configuration of effective sites. A unique feature of the developed MLR model is that a cross-validation is performed at each time step for each configuration of effective sites. Only relevant configurations (according to the RMSE and NS coefficient) are used. For example, using data from Sandy Hook (at which data is available from 1910) and Atlantic City (data available from 1911) the record at The Battery can be extended back to 1910 and data gaps filled in. As shown in Tables 1 and in the right panel of Fig. 2, time series at Sandy Hook and Atlantic City sites are quite long (more than 100 years). The configuration using observations at these two sites led to a relatively high NS and RMSE coefficients.

The ANOVA analysis led to consideration of all sites in the homogeneous region in the MLR model even when only Sandy Hook and Atlantic City sites, together or individually, are providing regional information (especially before 1938). These results suggest that more than 18,000 reconstituted values were used to enrich the initial at-site time series.

3.3.3. *TS-RFM results*

TS-RFM results at the Battery are presented in terms of estimates of the quantiles of interest (100-year, 500-year and 1 000-year return levels) and associated 70% and 90% CI. Optimal threshold values for the local SSS, MISS and MaxSL series at The Battery (NY) enriched with the regional information are obtained with the stability curves.

- A threshold of 0.89 m was obtained for SSS
- The same threshold was obtained for MISS
- A threshold of about 1.43 m was selected for MaxSL

After threshold selection, the effective record (in years) without the gaps was computed as the ratio between number of days with observations and the average number of days in a year (365.25).

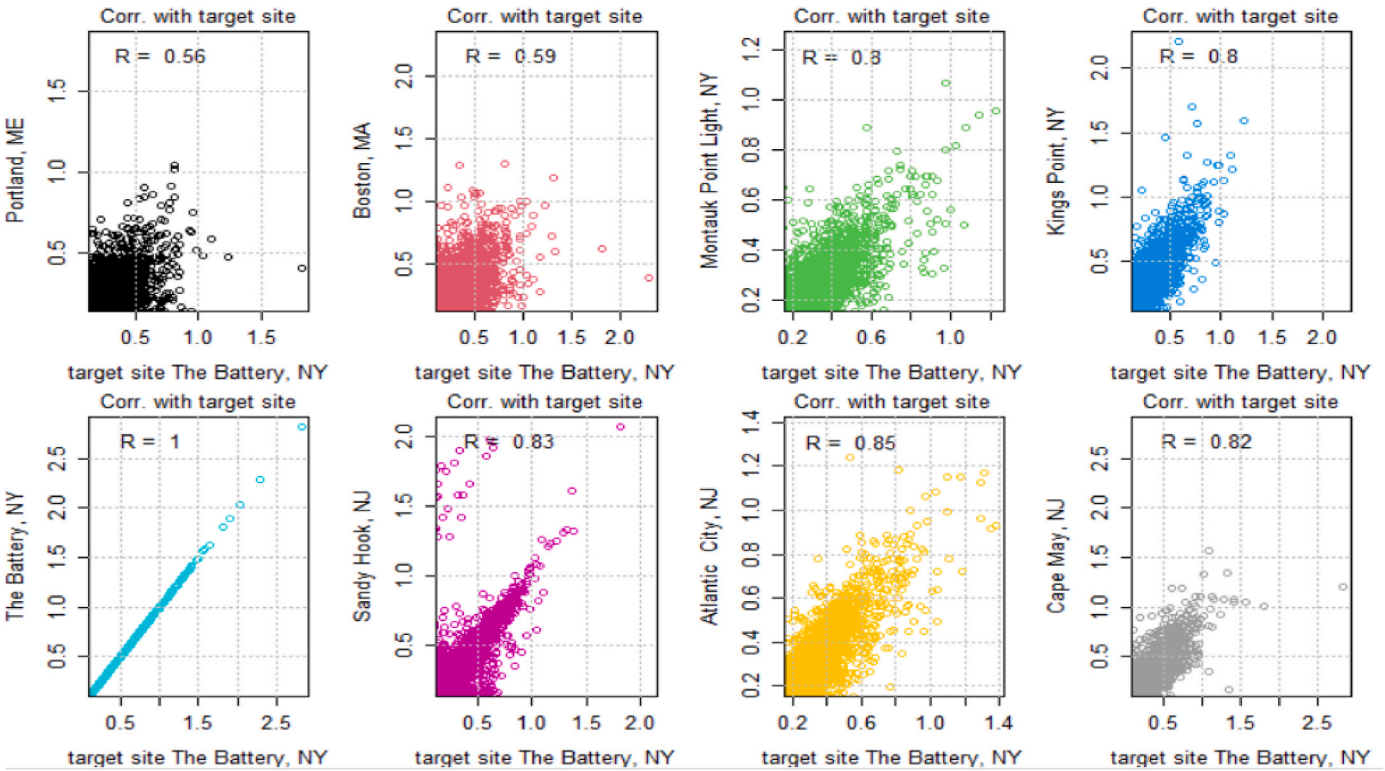

Fig. 6. MISS pairwise correlation between The Battery, NY (target site) and neighboring sites.

Comparison of GPD frequency estimation at The Battery, using SSS, MISS and MaxSL, with and without regional information included are presented in Fig. 7, and summarized in Tables 2 and 3. The empirical distribution is indicated by solid circles in the figures, while the fitted GPD distribution is shown by the solid line. The POT method settings and number of exceedances are presented in the tables. In all cases, the distribution shape parameter changed slightly, owing to the presence of added regional extreme surges in the central part of the distribution (i.e., increased probability mass), but not in the vicinity of the outlier, because there are no other similar magnitude events in the upper tail.

In addition to the fact that the POT approach with GPD fit naturally uses more extremes than the annual maximum series approach with a generalized extreme value distribution, typically leading to narrower CIs (e.g., Hamdi et al., 2014), there is less variability since the regional information is used to enlarge the sample size (e.g., increasing the effective record at The Battery, NY from 85 years to 102 years). We can observe in Tables 2 and 3 that the CIs became narrower only when regional information was added to the at-site MISSs. We also observe that the fit at the right tail of the distribution (excluding the outlier) is slightly better than that obtained with only local information. This illustrates the non-consistency of the regional extreme surges in the analysis when no exceptional surges or sea levels are found in the region of interest. Although the outlier is slightly better represented in the sample and is closer to the central body of the distribution, it has remained outside the CIs.

The inclusion of the regional information resulted in lowering the shape parameter and consequently lower quantiles are obtained for the desired return periods. The decreases at the Battery, NY are.

- SSS, 100-yr return level: 9 cm decrease (~5%)
- SSS, 1 000-yr return level: 29 cm decrease (~8%)
- MISS, 100-yr return level: 13 cm decrease (~5%)
- MISS, 1 000-yr return level: 32 cm decrease (~8%)
- MaxSL, 100-yr return level: 9 cm decrease (~3%)
- MaxSL, 1 000-yr return level: 14 cm decrease (~3%)

4. Discussion

In this section we compare inferences, for all variables of interest, resulting from the different approaches, focusing on TS-RFM with and without regional information, SST with and without monthly data, and JPM-AMP at a virtual gage. We compare estimates of 100-, 500- and 1 000-year return levels and assess uncertainty using the 70% and 90% CIs. Fitting performance is assessed by visually examining diagnostic plots. We provide a qualitative comparison based on the plots in Figs. 3 and 7, then discuss the numerical results in Tables 2 and 3 We compare inferences produced using the FA methods (TS-RFM and SST) and we also compare the FA results to those obtained using JPM-AMP.

Visual inspection of SST and TS-RFM local and extremogram-based regional model results (Figs. 3 and 7, respectively) shows that results depend on the variable of interest. Both approaches produce narrower CIs when additional information (i.e., regional, and monthly water levels) are included. This can be seen and comparing the bottom left and bottom right panels of Fig. 3 and by comparing left and right panels of Fig. 7.

Further visual inspection of Figs. 3 and 7 also provides some insight into hurricane Sandy, which is responsible for the storm surge of record for this location. The 70% and 90% CIs show that both TS-RFM and SST approaches indicate that the surge due to hurricane Sandy was not an extremely rare event. However, Sandy SSS and MaxSL exhibit outlier behavior, while the MISS/NTR is within the CIs. We attribute this difference to the arrival time of the surge relative to the astronomical tides (Sandy's surge coincided with high tide at the Battery). We also note that the "outlier" status is also a function of the plotting position formula. We used the Weibull formula, which is often used in extreme value analysis (Makkonen, 2006). Other plotting position formulas may produce different results. The MISS/NTR variables focus on the instantaneous peak surge (tide effects filtered out) while SSS and MaxSL are not isolated from tides. From the local and regional TS-RFM MaxSL plots (bottom panel of Fig. 7), we can visually estimate that the Sandy MaxSL was approximately a 1 in 400-year to 1 in 500-year event. The SST

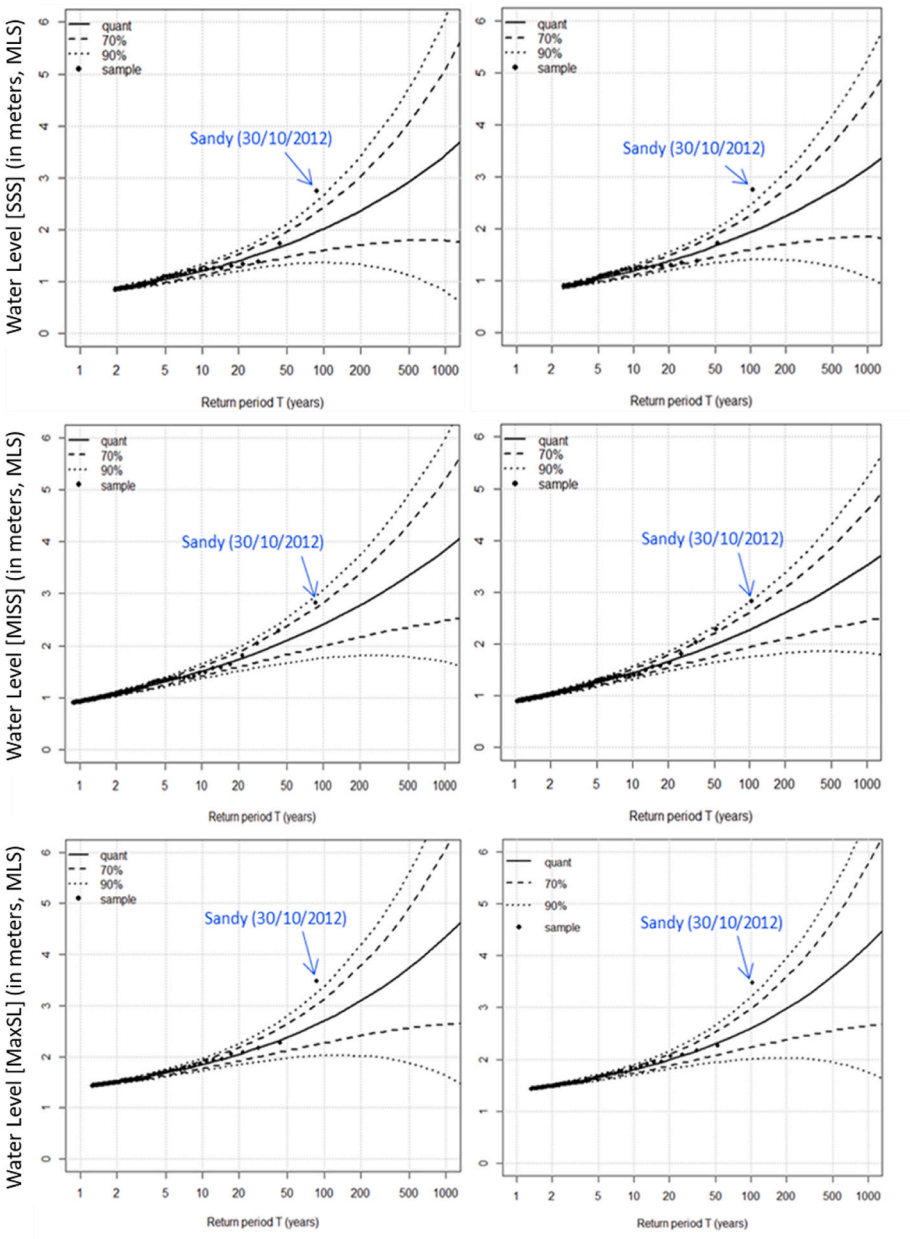

Fig. 7. TS-FRM GPD fits to storm surge data at the Battery (NY) with local information (left panels) and including regional data (right panels): (top) SSS; (middle) MISS; (bottom) MaxSL.

MaxSL plots (hourly and hourly plus monthly maxima; bottom panel of Fig. 3) infers an estimate of about 1 in 300 years to 1 in 1 000 years. However, it should be stressed that these estimates are very uncertain, as shown by the calculated CIs in the plots. Other studies have suggested that Sandy had the largest observed maxSL and second largest MISS in over 300 years (Orton et al., 2016).

Visual inspection of Fig. 4 shows that the JPM-AMP storm surge hazard curves are significantly different from the FA approaches both with respect to CIs and shape of the curves. The JPM-AMP CIs are more uniform over a wide AEF range and growth in the mean hazard with decreasing AEF is more modest compared to FA methods. This results from the very large number of storms which can be included using the gaussian process metamodeling approach. We note that the observed surge from Sandy falls within the JPM-AMP 90% CI. Visual inspection indicates provides an estimated return period of approximately 200 years for the observed the Sandy water level.

Table 2 shows statistical inference results using only local hourly data. We observe that the TS-RFM at-site FA and SST mean surge and water level estimates are similar for all variables. Results for SST are slightly lower than those for TS-RFM (about 1% lower for MaxSL and less than 6% lower for NTR/MISS). Although the mean surge and water level estimates are similar, the SST and TS-RFM approaches recover different number of POT exceedances (N). SST recovers about 40%, 170% and 250% more exceedances for MaxSL, NTR/MISS, and SSS, respectively. The difference in exceedances is attributed mainly to differences in thresholds used to estimate the frequency model shape and scale parameters, with SST thresholds consistently lower than TS-RFM.

Table 2 also shows that the SST method with only hourly data produces narrower CIs than the TS-RFM at-site FA method (about 20–40% lower for NTR/MISS and approximately 7%–20% lower for MaxSL for both the 70% and 90% CIs). The difference grows with increasing return period. As was stated previously, TS-RFM uses relatively higher thresholds to extract extreme events. Consequently, the smaller sample size leads to wider CIs. The SST CIs are obtained by bootstrapping, while

Table 2
The Battery, NY - Results of the at-site TS-RFM (without regional information) and SST with hourly data: 100-, 500- and 1 000-year return levels and their 70% and 90% confidence intervals.

The Battery, NY: with hourly local information only						
	SSS		NTR & MISS		MaxSL	
	SST	TS-RFM	SST	TS-RFM	SST	TS-RFM
Record length	94	94	94	94	94	94
D_{eff}	85.53	85.57	85.53	85.87	85.53	85.57
u_{POT} *(m)*	0.62	0.85	0.77	0.9	1.42	1.43
N	161	45	272	98	98	69
RL_{100} *(70%CI)*	2.02 (1.63–2.41) 39%	2.02 (1.61–2.43)	2.42 (2.09–2.73)	2.41 (2.00–2.82)	2.74 (2.34–3.14) 29%	2.70 (2.27–3.13)
$\Delta s/\ s$ (%)		41%	26%	34%		32%
RL_{500}*(70%CI)*	2.79 (1.96–3.62)	2.93 (1.79–4.06)	3.20 (2.54–3.81)	3.33 (2.36–4.31)	3.72 (2.72–4.70) 53%	3.74 (2.57–4.91)
$\Delta s/\ s$ (%)	59%	77%	40%	59%		63%
RL_{1000}*(70%CI)*	3.21 (2.10–4.33)	3.44 (1.79–5.09)	3.60 (2.74–4.42)	3.83 (2.48–5.18)	4.31 (2.89–5.69) 65%	4.35 (2.64–6.07)
$\Delta s/\ s$ (%)	69%	96%	47%	70%		79%
RL_{100}*(90%CI)*	2.02 (1.50–2.74)	2.02 (1.36–2.67)	2.42 (1.96–2.97)	2.41 (1.76–3.07)	2.74 (2.21–3.48) 46%	2.70 (2.02–3.38)
$\Delta s/\ s$ (%)	61%	65%	42%	54%		50%
RL_{500}*(90%CI)*	2.79 (1.72–4.43)	2.93 (1.13–4.72)	3.20 (2.32–4.35)	3.34 (1.79–4.88)	3.72 (2.49–5.73) 87%	3.74 (1.88–5.60)
$\Delta s/\ s$ (%)	97%	122%	63%	92%		99%
RL_{1000}*(90%CI)*	3.21 (1.81–5.46)	3.44 (0.82–6.06)	3.60 (2.47–5.15)	3.83 (1.69–5.97)	4.31 (2.59–7.33)	4.35 (1.63–7.08)
$\Delta s/\ s$ (%)	114%	152%	74%	112%	110%	125%

Table 3
The Battery, NY - Results of the TS-RFM with regional information included, SST with hourly and monthly data, and JPM-AMP: 100-, 500- and 1 000-year return levels and their 70% and 90% confidence intervals.

The Battery, NY: IRSN results with regional information; USACE SST results with monthly local information; and USACE JPM-AMP results from CHS-NA-2023 at virtual gage 230,889.						
	SSS	NTR & MISS		MaxSL		
	TS-RFM with regional	JPM-AMP	TS-RFM with regional	SST with monthly maxima	JPM-AMP	TS-RFM with regional
Rec. length	n/a	n/a	n/a	121	n/a	n/a
D_{eff}	102	n/a	102	118.69	n/a	102
u_{POT} *(m)*	0.89	n/a	0.89	1.41	n/a	1.43
N	41	n/a	100	181	n/a	78
RL_{100} *(70%CI)*	1.93 (1.60–2.26)	2.87 (2.27–3.48)	2.28 (1.94–2.61)	2.52 (2.25–2.78)	3.11 (2.49–3.72)	2.61 (2.23–2.98)
$\Delta s/\ s$ (%)	34%	42%	29%	21%	39%	29%
RL_{500}*(70%CI)*	2.72 (1.81–3.62)	3.83 (3.20–4.45)	3.09 (2.31–3.86)	3.15 (2.57–3.72)	3.86 (3.23–4.48)	3.61 (2.56–4.66)
$\Delta s/\ s$ (%)	66%	33%	50%	37%	32%	58%
RL_{1000}*(70%CI)*	3.15 (1.84–4.47)	4.12 (3.49–4.75)	3.51 (2.45–4.58)	3.49 (2.72–4.24)	4.09 (3.46–4.72)	4.21 (2.66–5.76)
$\Delta s/\ s$ (%)	83%	30%	61%	44%	31%	74%
RL_{100}*(90%CI)*	1.93 (1.40–2.46)	2.87 (1.92–3.83)	2.28 (1.75–2.81)	2.52 (2.17–3.02)	3.11 (2.14–4.07)	2.61 (2.01–3.20)
$\Delta s/\ s$ (%)	55%	67%	45%	34%	62%	45%
RL_{500}*(90%CI)*	2.72 (1.28–4.15)	3.83 (2.84–4.82)	3.09 (1.86–4.32)	3.15 (2.41–4.31)	3.86 (2.86–4.85)	3.61 (1.94–5.27)
$\Delta s/\ s$ (%)	105%	52%	80%	60%	51%	92%
RL_{1000}*(90%CI)*	3.15 (1.07–5.24)	4.12 (3.13–5.12)	3.51 (1.83–5.20)	3.49 (2.51–5.13)	4.09 (3.10–5.09)	4.21 (1.75–6.68)
$\Delta s/\ s$ (%)	132%	48%	96%	75%	49%	117%

those of TS-RFM are based on a Gaussian assumption (delta method), which is more sensitive to the number of exceedances.

We now pivot to discussing the effect of including additional information. Table 3 shows results when including additional information: (1) TS-RFM with regional information; (2) SST with monthly maxima; and (3) JPM-AMP using synthetic storms. Note that monthly maxima are only available for MaxSL. In general, comparing results between Tables 2 and 3, we observe that including additional information reduces uncertainty, as expected.

For TS-RFM, regionalization slightly reduces the mean surge and water level estimates by about 3%–8% (the reduction grows with return period for surge, but not for water level). Regionalization reduces the 70% and 90% CIs for SSS and NTR/MISS by approximately 20%. For MaxSL the 70% and 90% CIs are reduced by about 10%. These results do not appear to be sensitive to return period.

For SST, inclusion of monthly water level data reduces the mean water level estimates by 8%–20%, with larger reductions at longer return periods. Uncertainty is reduced, as expected, with results varying with return period. Including monthly water level data reduces the 70% CIs by approximately 34%, 42% and 46% for the 100-, 500- and 1 000-yr return periods, respectively. Similar reductions are obtained for the 90% CIs.

Comparing the TS-RFM regional model results to those for SST with monthly maxima, we observe that SST water level estimates are about 3–20% lower, and the CIs are 35–40% narrower. These differences grow with increasing return period.

Comparing the TS-RFM regional model to JPM-AMP, we observed that JPM-AMP NTR/MISS and MaxSL results are generally higher than those for TS-RFM (about 25% and 20 % higher at 100 years, respectively), but the differences decrease with increasing return period. At the 100-year return period, the JPM-AMP CIs are consistently wider, but TS-RFM CIs grow much faster than JPM-AMP with longer return periods. These differences are mainly a function of the large number of simulated storms included in JPM-AMP analyses. JPM-AMP hazards curves are typically flatter and slightly concave down compared to concave up curves typical of frequency analysis approaches.

5. Conclusions and perspectives

The main objective of this work was to compare and contrast IRSN and USACE storm surge statistical and probabilistic modeling approaches. The methods were applied to a U.S. North Atlantic coast location (The Battery, NY) that is subject to both tropical and extratropical storm surge phenomena. Results compared include magnitudes

and frequency (AEF), uncertainties, and visual examination of fitting quality for the following explanatory variables: skew surge, maximum instantaneous surge, non-tidal residual, and maximum sea level. The IRSN TS-RFM method computes at-site frequency estimates by enriching the local time series with information from a homogeneous region around the target site. The USACE SST method enriches at-site data with monthly observations to extend the period of record. Although the two approaches differ and extract extreme values differently, the resulting samples are generally similar for both storm surge and water levels.

For local analysis at the Battery, the TS-RFM produces larger mean surge (approximately 4–8% for SSS and NTR/MISS), than SST at 500- and 1 000-year return levels. Differences in MaxSL were negligible (about 3%) at these return levels. In term of uncertainty quantification, the at-site results show that SST method produced narrower relative confidence intervals than TS-RFM, for all variables of interest. Both approaches indicate that surge and water levels for Hurricane Sandy are statistical outliers within the available record. When using the Weibull plotting position formula, observations from Sandy do not fit within the 90% CI for either approach for the SSS and MaxSL variables.

For both IRSN and USACE approaches, uncertainty is reduced when the analysis is performed in a regional context (TS-RFM with regional information, SST with monthly maxima, JPM-AMP using synthetic storms). When regional information is included, the JPM-AMP method produces higher mean surge than SST and the TS-RFM methods for NTR/MISS and MaxSL. TS-RFM mean surge is slightly higher than SST. Similar to the at-site results, SST confidence intervals are consistently narrower than the TS-RFM. The JPM-AMP CIs grow more slowly with return period relative to the other methods. We note that this study only used systematic observations (i.e., tide gage record), while the TS-RFM method can incorporate historical information predating systematic observations, which could further reduce uncertainties for the FA approach.

Overall, we found that results of the comparison of the IRSN and USACE methods vary with the variable of interest and return period. The TS-RFM and SST methods produce broadly similar estimates of surge and water level, but the confidence intervals for SST are systematically narrower and the difference increased with longer return periods. The JPM-AMP method produces higher water level estimates than the other methods (the difference decreases with increasing return period) and the growth of the JPM-AMP CIs with return period is significantly slower than the other methods. Although there are appreciable differences between the results documented in this paper, these are reasonable due to differences in the data and methods used in this comparison.

Funding

This research did not receive any specific grant from funding agencies in the public, commercial, or not-for-profit sectors.

Statement

During the preparation of this work the author(s) used the Renext R package in order to conduct the statistical inferences for the IRSN model. After using this package, the author(s) reviewed and edited the content as needed and take(s) full responsibility for the content of the publication.

CRediT authorship contribution statement

Yasser Hamdi: Conceptualization, Methodology, Writing – original draft, Calculations. **Norberto C. Nadal-Caraballo:** Data curation, Methodology, Calculations, Writing, Visualization, Writing – review & editing. **Joseph Kanney:** Supervision, Visualization, Writing – review & editing. **Meredith L. Carr:** Calculations, Writing, Visualization, Writing – review & editing. **Vincent Rebour:** Supervision, Writing – review & editing.

Declaration of competing interest

The authors declare that they have no known competing financial interests or personal relationships that could have appeared to influence the work reported in this paper.

Data availability

The authors do not have permission to share data.

Acknowledgements

USACE's contribution to this study were funded in part by the Coastal Hazards System (CHS) program.

References

Aerts, J.C.J.H., Lin, N., Botzen, W., Emanuel, K., de Moel, H., 2013. Low-probability flood risk modeling for New York city. Risk Anal. 33, 772–788. https://doi.org/10.1111/risa.12008.

Bardet, L., Duluc, C.-M., Rebour, V., 2011. Regional frequency analysis of extreme storm surges along the French coast. Nat. Hazards Earth Syst. Sci. 11, 1627–1639. https://doi.org/10.5194/nhess-11-1627-2011.

Blake, E.S., Kimberlain, T.B., Berg, R.J., 2013. Tropical Cyclone Report - Hurricane Sandy (AL182012) 22–29 October 2012. National Hurricane Center.

Blake, E.S., Zelinksy, D.A., 2018. Tropical Cyclone Report - Hurricane Harvey (AL092017) 17 August – 1 September 2017. National Hurricane Center.

Bucci, L., Alaka, L., Hagen, A., Delgado, S., Beven, J., 2023. Tropical Cyclone Report - Hurricane Ian (AL092022) 23–30 September 2022. National Hurricane Center.

Coles, S., 2001. An introduction to statistical modeling of extreme values. In: Lecture Notes in Control and Information Sciences. Springer.

Gonzalez, V.M., Nadal-Caraballo, N.C., Melby, J.A., Cialone, M.A., 2019. Quantification of uncertainty in probabilistic storm surge models: literature review. In: ERDC/CHL SR-19-1. Vicksburg, MS. US Army Engineer Research and Development Center.

Hall, T.M., Jewson, S., 2007. Statistical modeling of North Atlantic tropical cyclone tracks. Tellus 59A, 486–498. https://doi.org/10.1111/j.1600-0870.2007.00240.x.

Hamdi, Y., Bardet, L., Duluc, C.-M., et al., 2014. Extreme storm surges: a comparative study of frequency analysis approaches. Nat. Hazards Earth Syst. Sci. 14, 2053–2067. https://doi.org/10.5194/nhess-14-2053-2014, 2014.

Hamdi, Y., Bardet, L., Duluc, C.-M., et al., 2015. Use of historical information in extreme-surge frequency estimation: the case of marine flooding on the La Rochelle site in France. Nat. Hazards Earth Syst. Sci. 15, 1515–1531. https://doi.org/10.5194/nhess-15-1515-2015, 2015.

Hamdi, Y., Garnier, E., Giloy, N., Duluc, C.-M., et al., 2018. Analysis of the risk associated with coastal flooding hazards: a new historical extreme storm surges dataset for Dunkirk, France. Nat. Hazards Earth Syst. Sci. 18, 3383–3402. https://doi.org/10.5194/nhess-18-3383-2018.

Hamdi, Y., Duluc, C.-M., Bardet, L., et al., 2019. Development of a target-site-based regional frequency model using historical information. Nat. Hazards 98, 895–913. https://doi.org/10.1007/s11069-018-3237-8.

IRSN, Alpstat, 2013. Renext: Renewal Method for Extreme Values Extrapolation. http://cran.r-project.org/web/packages/Renext/.

Jia, G., Taflanidis, A.A., Nadal-Caraballo, N.C., Melby, J.A., 2016. Surrogate modeling for peak or time-dependent storm surge prediction over an extended coastal region using an existing database of synthetic storms. Nat. Hazards 81, 909–938.

Knobby, R.D., Rhome, J.R., Brown, D.P., 2023. Hurricane Katrina. National Hurricane Center Tropical Cyclone Report AL12205.

Langousis, A., Mamalakis, A., Puliga, M., Deidda, R., 2016. Threshold detection for the generalized Pareto distribution: review of representative methods and application to the NOAA NCDC daily rainfall database. Water Resour. Res. 52, 2659–2681. https://doi.org/10.1002/2015WR018502.

Liberato, M.L.R., Pinto, J.G., Trigo, I.F., Trigo, R.M., 2011. Klaus – an exceptional winter storm over northern Iberia and southern France. Weather 66, 330–334. https://doi.org/10.1002/wea.755.

Liberato, M.L.R., Pinto, J.G., Trigo, R.M., Ludwig, P., Ordóñez, P., Yuen, D., Trigo, I.F., 2013. Explosive development of winter storm Xynthia over the subtropical North Atlantic ocean. Nat. Hazards Earth Syst. Sci. 13, 2239–2251. https://doi.org/10.5194/nhess-13-2239-2013.

Lin, N., Emanuel, K., Smith, J., Vanmarcke, E., 2010. Risk assessment of hurricane storm surge for New York City. J. Geophys. Res. Atmos. 115 https://doi.org/10.1029/2009JD013630.

Lin, N., Kopp, R., Horton, B., Donnelly, J., 2016. Hurricane Sandy's flood frequency increasing from year 1800 to 2100. Proc. Natl. Acad. Sci. USA 113 (43), 12071–12075. https://doi.org/10.1073/pnas.1604386113.

Makkonen, L., 2006. Plotting positions in extreme value analysis. J. Appl. Meteorol. Climatol. 45, 334–340. https://doi.org/10.1175/JAM2349.1.

Melby, J.A., Nadal-Caraballo, N.C., Pagan-Albelo, Y., Ebersole, B.A., 2012. Wave Height and Water Level Variability on Lakes Michigan and St. Clair. ERDC/CHL TR-12-23. U.S. Army Engineer Research and Development Center, Vicksburg, MS.

Nadal-Caraballo, N.C., Melby, J.A., Ebersole, B.A., 2012. Statistical Analysis and Storm Sampling Approach for Lakes Michigan and St. Clair. ERDC/CHL TR-12-19. Vicksburg, MS. U.S. Army Engineer Research and Development Center.

Nadal-Caraballo, N.C., Melby, J.A., 2014. North Atlantic Coast Comprehensive Study – Phase I: statistical analysis of historical extreme water levels with sea level change. In: ERDC/CHL TR-14-7. U.S. Army Engineer Research and Development Center, Vicksburg, MS.

Nadal-Caraballo, N.C., Melby, J.A., Gonzalez, V.M., Cox, A.T., 2015a. North Atlantic Coast Comprehensive Study – Coastal Storm Hazards from Virginia to Maine. ERDC/CHL TR-15-5. Vicksburg, MS. U.S. Army Engineer Research and Development Center.

Nadal-Caraballo, N.C., Melby, J.A., Gonzalez, V.M., 2015b. Statistical analysis of historical extreme water levels for the U.S. North Atlantic Coast using Monte Carlo Life-Cycle Simulation. J. Coast Res. 32 (1), 35–45. https://doi.org/10.2112/JCOASTRES-D-15-00031.1.

Nadal-Caraballo, N.C., Yawn, M.C., Aucoin, L.A., Carr, M.L., Melby, J.A., Ramos-Santiago, E., Gonzalez, V.M., Taflanidis, A.A., Kyprioti, A.A., Cobell, Z., Cox, A.T., 2022. Coastal Hazards System–Louisiana (CHS-LA). ERDC/CHL TR-22-16. Vicksburg, MS. US Army Engineer Research and Development Center. https://doi.org/10.21079/11681/45286.

Orton, P., Vinogradov, S., Georgas, N., Blumberg, A., Lin, N., Gornitz, V., Little, C., Jacob, K., Horton, R., 2015. New York city panel on climate change 2015 report chapter 4: dynamic coastal flood modeling. Ann. N. Y. Acad. Sci. 1336, 56–66. https://doi.org/10.1111/nyas.12589.

Orton, P.M., Hall, T.M., Talke, S.A., Blumberg, A.F., Georgas, N., Vinogradov, S., 2016. A validated tropical-extratropical flood hazard assessment for New York Harbor. J. Geophys. Res. Oceans 121, 8904–8929. https://doi.org/10.1002/2016JC011679.

Orton, P., Lin, N., Gornitz, V., Colle, B., Booth, J., Feng, K., Buchanan, M., Oppenheimer, M., Patrick, L., 2019. New York city panel on climate change 2019 report chapter 4: coastal flooding. Ann. N. Y. Acad. Sci. 1439 (1), 95–114. https://doi.org/10.1111/nyas.14011.

Pasch, R.J., Berg, R., Roberts, D.P., Papin, P.P., 2021. Tropical Cyclone Report - Hurricane Laura (AL132020) 20–29 August 2020. National Hurricane Center.

Pasch, R.J., Penny, A.B., Berg, R., 2023. Tropical Cyclone Report - Hurricane Maria (AL152017) 16–30 September 2017. National Hurricane Center.

Pickands, J., 1975. Statistical inference using extreme order statistics. Ann. Stat. 3, 119–131. https://doi.org/10.1214/aos/1176343003.

Rumpf, J., Weindl, H., Höppe, P., Rauch, E., Schmidt, V., 2007. Stochastic modelling of tropical cyclone tracks. Math. Methods Oper. Res. 66, 475–490. https://doi.org/10.1007/s00186-007-0168-7.

Saint-Criq, L., Gaume, E., Hamdi, Y., Ouarda, T.B.M.J., 2022. Extreme sea level estimation combining systematic observed skew surges and historical record sea levels. Water Resour. Res. 58, e2021WR030873 https://doi.org/10.1029/2021WR030873.

Ulbrich, U., Fink, A.H., Klawa, M., Pinto, J.G., 2001. Three extreme storms over europe in december 1999. Weather 56, 70–80. https://doi.org/10.1002/j.1477-8696.2001.tb06540.x.

U.S. Army Corps of Engineers (USACE), 2009. Louisiana coastal protection and restoration (LACPR). In: Final Technical Report. New Orleans District, Mississippi Valley Division, New Orleans, LA.

USACE, 2011. Flood Insurance Study: Coastal Counties, Texas: Scoping and Data Review. Federal Emergency Management Agency, Denton, TX. Region 6.

Vickery, P., Skerlj, P., Twisdale, L., 2000. Simulation of hurricane risk in the U.S. Using empirical track model. J. Struct. Eng. 126 (10), 1222–1237.

Yawn, M.C., Nadal-Caraballo, N.C., Aucoin, L.A., Carr, M.L., Ramos-Santiago, E., Melby, J.M., Gonzalez, V.M., Massey, T.C., Owensby, M.B., Taflanidis, A.A., Kyprioti, A.P., Cox, A.T., 2023. Coastal Hazards System–South Atlantic (CHS-SA). ERDC/CHL TR-23-X. U.S. Army Engineer Research and Development Center, Vicksburg, MS (in press).

Yin, J., Yu, D., Lin, N., Wilby, R., 2017. Evaluating the cascading impacts of sea level rise and coastal flooding on emergency response spatial accessibility in Lower Manhattan, New York City. J. Hydrol. 555, 648–658.

Zhang, J., Taflanidis, A.A., Nadal-Caraballo, N.C., et al., 2018. Advances in surrogate modeling for storm surge prediction: storm selection and addressing characteristics related to climate change. Nat. Hazards 94, 1225–1253. https://doi.org/10.1007/s11069-018-3470-1.

Zhang, L., Singh, V.P., 2019. Copulas and Their Applications in Water Resources Engineering. Cambridge University Press, Cambridge.